Journal of Alloys and Compounds 473 (2009) 330–335

Contents lists available at ScienceDirect

Journal of Alloys and Compounds

journal homepage: www.elsevier.com/locate/jallcom

Investigation of dielectric and piezoelectric properties of niobium-modified PLSZFT nanoceramics for sensor and actuator applications

Koduri Ramam[a,*], A.J. Bell[b], C.R. Bowen[c], K. Chandramouli[d]

[a] Departmento de Ingeneria de Materials (DIMAT), Facultad de Ingenieria, Universidad de Concepcion, Concepcion, Chile
[b] Institute for Materials Research, University of Leeds, Leeds LS2 9JT, United Kingdom
[c] Materials Research Centre, Department of Mechanical Engineering, University of Bath, Bath BA2 7AY, United Kingdom
[d] Solid State Physics & Materials Research Laboratories, Department of Physics, Andhra University, Visakhapatnam, India

ARTICLE INFO

Article history:
Received 30 April 2008
Received in revised form 22 May 2008
Accepted 22 May 2008
Available online 9 July 2008

Keywords:
PLZT
Ferroelectrics
Dielectric response
Piezoelectrics

ABSTRACT

In this paper, the microstructure, dielectric and piezoelectric properties of pentavalent Nb^{5+} on isovalent Sr^{2+} and acceptor Fe^{3+}-modified PLZT have been reported. Nanocrystalline ceramic compositions $[Pb_{0.973}La_{0.012}Sr_{0.015}][(Zr_{0.54}Ti_{0.46})_{0.9895-(5n/4)}Fe_{0.01}Nb_n]O_3$ (PLSZFNT) where $n = 0$, 0.2, 0.4, 0.6, 0.8 and 1 mol%) near morphotrophic phase boundary were fabricated through solid-state reaction method.

X-ray diffraction patterns indicated that pure PLZT showed the presence of rhombohedral phase, and Fe and Sr incorporation into PLZT (PLSZFT) lattice shifted to coexistence of both rhombohedral and tetragonal phases while increasing Nb content in PLSZFT resulted in enhanced tetragonality. The tolerance factor ($t = 1.00$) indicates an ideal and stable tetragonal structure of PLSZFNT lattice. Grain size and apparent density were maximum at $Nb_{0.01}$. TEM studies indicated that average particle size ranged from 16 to 63 nm. The effect of grain growth on dielectric and piezoelectric properties were studied. The optimum dielectric and piezoelectric properties were found ($\varepsilon_{RT} = 2862$, $d_{33} = 491$ pC/N and $k_p = 0.522$) in $n = 1$ mol%, respectively, which could be suitable for possible sensor and actuator applications.

1. Introduction

Lead lanthanum zirconium niobate $Pb_{1-x}La_x(Zr_zTi_{1-z})_{1-x/4}O_3$, designated as PLZT belongs to the family of lead-based relaxor ferroelectrics and different cations could be doped both on the A-site and B-site of perovskite structure for outstanding dielectric and electromechanical properties. It has a relatively high ferroelectric phase transition temperature being around ≈340 °C at 1 kHz. PLZT compounds with particular compositions manifest a rather large value of piezoelectric effect. This feature makes them important for sensor and actuator applications. Perovskite-structured PLZT is also important for researchers engaged in investigations of fundamental and functional properties of solids due to a variety of phase transitions possible in these substances. These materials are also known for their unusual phase boundary, called the morphotrophic phase boundary (MPB) [1], which occurs at around $x \approx 53$ which separates two structural phases rhombohedral (zirconium-rich region) and tetragonal (titanium-rich region) structures; in particular, a very high dielectric and piezoelectric response is recorded in and around the MPB. The occurrence of the MPB depends mainly on the Zr:Ti ratio, dopants and procedure of preparation of the samples [2,3] and the structural modification influences the functional properties of polycrystalline materials. Multiple ions occupation of A and/or B sites in ABO_3 compounds can influence the lattice parameters; as a consequence, a change in the physical and functional properties is expected due to the polarization [4].

High power or "hard" piezoelectric ceramics can withstand high levels of electrical excitation and mechanical stress. These materials are suited for high voltage or high power generators and transducers. Hard piezoelectric ceramics are more resistant to stress-induced depolarization compared to soft piezoelectrics. Hard piezoelectric materials are characterized by a very high load or distortion constant, low hysteresis and high Q_m. Whereas, soft piezoelectrics are less resistant to stress induced depolarization compared to hard piezoelectrics. "Soft" ceramics feature high sensitivity and permittivity, but if over driven these materials can be damaged due to self-heating beyond their operating temperature range or Curie temperature. Soft piezoelectrics are used in various sensors, low-power motor-type transducers, receivers, and low power generators. An ideal piezoelectric ceramic could be the combination of both hard (acceptor) and soft (donor) dopants near the morphotrophic phase boundary which could be resistive as well as sensitive. Previous investigations reported that high electromechanical behaviour was found with soft doping (isovalent Ba [5]

* Corresponding author. Tel.: +56 41 2203369; fax: +56 41 2739800.
E-mail address: ramamk@udec.cl (K. Ramam).

0925-8388/$ – see front matter © 2008 Elsevier B.V. All rights reserved.
doi:10.1016/j.jallcom.2008.05.092

and Sr [6,7]) and hard doping (acceptors Ag [8] and Fe [9,10]). The electrical and mechanical properties of donor and/or acceptor-modified PLZT depends on the nature of dopant, its concentration and its effects in stoichiometric compounds resulting in desired end products which influence the microstructure, being this a consequence of the processing route. The properties of the ceramics for any specific application desired can be achieved by using element substitution.

PLZT has been extensively investigated for different dopants by many researchers. However, the combination of isovalent Sr, acceptor Fe and donor Nb (PLSZFNT, 1.2/1.5/54/1/Nb_n/46) has not been reported in the literature. Moreover, this system includes donor, isovalent and acceptor dopants which are expected to enhance the dielectric and piezoelectric properties. Also, there is no consensus on mechanisms determining the nature or influence of these dopants on dielectric and piezoelectric properties of the ceramic system. The objective of this study is to investigate the combinatory influence of donor, isovalent and acceptor dopants for enhanced dielectric and piezoelectric properties and to study the compositional dependence of donor Nb^{5+}-modified PLSZFT nanoceramics. The stoichiometric compositions are given in Table 1.

2. Experimental procedure

2.1. Ceramic processing

Analytical grade (99.99% purity) PbO, La_2O_3, $SrCO_3$, ZrO_2, Fe_2O_3, TiO_2 and Nb_2O_5 powders were mixed with excess 5 wt% (optimized) PbO to form PLSZFNT. The detailed fabrication of ceramics is reported elsewhere [5,10]. The batch powders were ball-milled (zirconia balls and ethanol as media for 24 h) and calcined (925 °C for 3 h) in a high purity alumina crucible. Calcined powders were ball-milled (zirconia balls and ethanol as media for 24 h) to crush agglomerates and to minimize the particle size. The calcined fine powders were mixed with 5 wt% polyvinyl alcohol (PVA, as binder) and were pressed into pellets (12 mm diameter and 2–3 mm thickness) using steel die and hydraulic press with uniaxial pressure of 700–900 kg/cm^2. Binder was burned off at 500 °C for 3 h and the green bodies were sintered at 1250 °C for 3 h. The sintering process was conducted in a lead-rich environment and fired in closed alumina crucibles to minimize lead oxide volatilization. After sintering process, the samples were cooled to the room temperature in furnace.

2.2. Structural characterization

The sintered specimens were characterized for phase formation by Philips X-ray diffractometer for sintered specimens (PW-1710, Cu Kα radiation, Ni filter, 1°/min). JEOL JSM 840A scanning electron microscopy was used to analyze microstructure of polished, etched and fractured ceramic surfaces. The scanning electron micrographs were analyzed by linear interception method for grain sizes. JEOL JEM 1200 transmission electron microscope was used to analyze particle size of the calcined powders.

2.3. Dielectric and piezoelectric characterization

Electroded specimens were characterized for dielectric properties (ε_{RT}, ε_{Tc}, T_c and tan δ) by using HP-4192A Impedance Analyzer at 1 kHz. Dielectric loss D is a significant factor and is usually equal to the ratio of effective series resistance to the effective reactance. It is the tangent of the loss angle and is given by the formula.

$$D = \tan\delta = \frac{\text{series resistance}}{\text{series reactance}}$$

The dielectric constant is calculated from the following formula:

$$\varepsilon = \frac{cd}{\varepsilon_0 A}$$

where c is the capacitance, d is the thickness, A is the surface area of sample and ε_0 is the permittivity of free space = 8.85×10^{-12} Farad/meter. Electroded specimens were poled in silicon oil bath at 100 °C by applying a dc field of 20 kV/cm. The piezoelectric charge coefficients (d_{33}) were characterized using a Berlincourt piezo-d-meter. The piezoelectric planar coupling coefficient (k_p) was characterized as follows—as per the IRE standards on piezoelectric crystals: measurements of piezoelectric ceramics, the following formula has been employed to find out piezoelectric planar coupling coefficient (k_p):

$$\frac{k_p^2}{1-k_p^2} = 2.51 \times \left[\frac{f_a - f_r}{f_r}\right]$$

where k_p = piezoelectric planar coupling coefficient, f_r = resonance frequency and f_a = anti-resonance frequency of poled ceramic. The resonance (f_r) and anti-resonance (f_a) frequencies of poled samples were measured by using a 4192A HP impedance analyzer.

3. Results and discussion

3.1. XRD studies of undoped and Nb-modified PLSZFT nanoceramics

Fig. 1 represents X-ray diffraction patterns of undoped and Nb-modified PLSZFT nanoceramics. It has been observed that pure PLZT (1.2/54/46) showed the presence of rhombohedral phase. The incorporation of isovalent Sr^{2+} and acceptor Fe^{3+} shifted the rhombohedral phase to coexistence with both rhombohedral and tetragonal phases. The initial incorporation of Nb content (0.2 mol%) resulted in coexistence of FE_{RH} (ferroelectric rhombohedral) and FE_{TET} (ferroelectric tetragonal) phases and further Nb content (0.4 mol%) increment shifted the coexistence to tetragonal phase. The tetragonality increased as Nb content increased in PLSZFT lattice. The tetragonal phase with peak splittings at (0 0 2) and (2 0 0), and (1 1 2) and (2 1 1), respectively, can be observed in Fig. 1, and the tetragonality could be ascribed to Sr, Fe and Nb content in PLZT lattice. The donor La^{3+} (R_{La} = 1.36 Å) and isovalent Sr^{2+} (R_{Sr} = 1.44 Å) occupies the A-site of PZT lattice partially substituting Pb^{2+} (R_{Pb} = 1.49 Å), while the acceptor Fe^{3+} (R_{Fe} = 0.645 Å) and donor Nb^{5+} (R_{Nb} = 0.64 Å) occupies the B-site of PZT lattice owing to the similar ionic radius of Zr^{4+} (R_{Zr} = 0.72 Å) and Ti^{4+} (R_{Ti} = 0.605 Å) [11]. The co-existence of tetragonal and rhombohedral phases is found in PLZT ceramics at or near MPB and phase stability depends on the dopant nature, type and concentrations [12]. In our study, the increasing Nb content resulted in phase transition from coexistence to tetragonal phase. The location of the MPB composition range is displaced towards titanium-rich end enhancing the tetragonality in the lattice due to the incorporation of Nb^{5+} into B-site of PLSZFT perovskite structure while stabilizing tetragonal phase against rhombohedral phase [13].

3.2. Tolerance factor

ABO_3-structured perovskite has different types of ferroic phases including ferroelectrics, antiferroelectrics, ferroeleastics, ferromagnetics and coupled forms of these phases. Using the relation

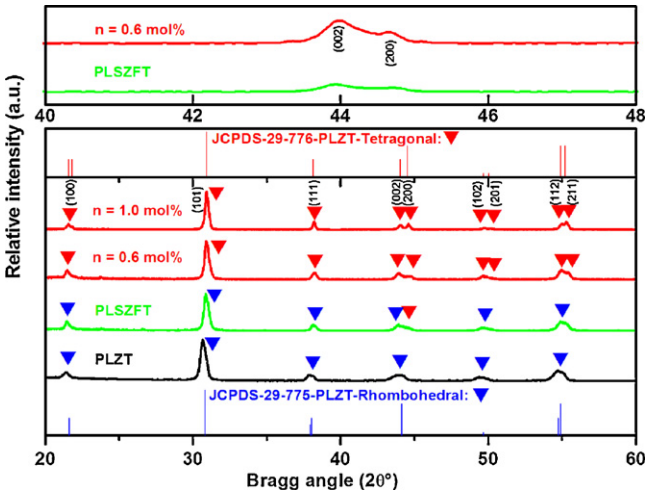

Fig. 1. X-ray diffraction patterns of undoped and Nb-modified PLSZFT nanoceramics.

Table 1
PLSZFNT nanoceramics synthesized

S.N.	Composition	Formulae
1	General formula	$[Pb_{1-x-y}La_xSr_y][(Zr_zTi_{1-z})_{(1-(x/4)-(3f/4)-(5n/4))}Fe_fNb_n]O_3$ (PLSZFNT)
2	Chemical formula	$[Pb_{0.973}La_{0.012}Sr_{0.015}][(Zr_{0.54}Ti_{0.46})_{0.9895-(5n/4)}Fe_{0.01}Nb_n]O_3$
		x = La = 1.2 mol% = 0.012, y = Sr = 1.5 mol% = 0.015, z = Zr = 54 mol% = 0.54, $1-z$ = Ti = 46 mol% = 0.46, f = Fe = 1 mol% = 0.01, n = Nb = 0–1 mol%
3	PLZT	$[Pb_{0.988}La_{0.012}][(Zr_{0.54}Ti_{0.46})_{0.997}]O_3$
4	PLSZFT, n = 0 mol%	$[Pb_{0.973}La_{0.012}Sr_{0.015}][(Zr_{0.54}Ti_{0.46})_{0.9895}Fe_{0.01}]O_3$
5	PLSZFT, n = 0.2 mol%	$[Pb_{0.973}La_{0.012}Sr_{0.015}][(Zr_{0.54}Ti_{0.46})_{0.987}Fe_{0.01}Nb_{0.002}]O_3$
6	PLSZFT, n = 0.4 mol%	$[Pb_{0.973}La_{0.012}Sr_{0.015}][(Zr_{0.54}Ti_{0.46})_{0.9845}Fe_{0.01}Nb_{0.004}]O_3$
7	PLSZFT, n = 0.6 mol%	$[Pb_{0.973}La_{0.012}Sr_{0.015}][(Zr_{0.54}Ti_{0.46})_{0.982}Fe_{0.01}Nb_{0.006}]O_3$
8	PLSZFT, n = 0.8 mol%	$[Pb_{0.973}La_{0.012}Sr_{0.015}][(Zr_{0.54}Ti_{0.46})_{0.9795}Fe_{0.01}Nb_{0.008}]O_3$
9	PLSZFT, n = 1 mol%	$[Pb_{0.973}La_{0.012}Sr_{0.015}][(Zr_{0.54}Ti_{0.46})_{0.977}Fe_{0.01}Nb_{0.01}]O_3$

for perovskite structural tolerance factor (t):

$$t = \frac{r_A + r_X}{\sqrt{2}(r_B + r_X)}$$

where r_A = ionic radii of A-site cations, r_B = ionic radii of B-site cation, r_X = ionic radii of anion [14], the stability of the perovskite phase in the perovskite family can be determined. Complex perovskite with ordered mixed species on a site (particularly the B-site) may be represented by multiples of this formula unit and larger unit cells. The A-site is a 12-coordinated cubo-octahedral hole in the oxygen network that is equivalent to an oxygen vacancy and is most readily occupied by large ions with crystal radii greater than or equal to that of O^{2-} (1.26) [11]. The B-site is a 6-coordinated octahedral site typically occupied by smaller ions. The structure may be viewed as AO_3 cubic close-packing with B ions occupying the octahedral voids and is therefore atomically dense. When t is equal to 1, the packing is said to be ideal. When t is larger than 1, there is too large a space available for B ion, and therefore this ion can move inside its octahedron. In general, to form a stable perovskite structure, one requires that $0.9 < t < 1.1$. Roth [15] had made a detailed classification of A^{2+}, B^{4+} and O_3^{2-} compounds. The tolerance factor for the synthesized compositions has been represented in Table 2. As can be evidenced from Table 2, PLZT and PLSZFNT compositions are more stable with ferroelectric rhombohedral and ferroelectric tetragonal phases, respectively, while PLSZFT (undoped) with coexistence of both FE_{RH} and FE_{TET} phases has some distortions in the lattice. PLSZFNT compositions exhibited a tolerance factor of 1.00 which is an ideal ferroelectric tetragonal structure which confirmed the stability in the perovskite ferroelectric tetragonal phase and supported by XRD studies.

3.3. Microstructure and apparent density profile of undoped and Nb-modified PLSZFT nanoceramics

Fig. 2 shows average grain size variation and apparent density of undoped and Nb-modified PLSZFT nanoceramics. Fig. 3(a–d) shows scanning electron micrographs (fractured surfaces) of 0.2, 0.4, 0.6 and 1 mol% Nb-modified PLSZFT, respectively, and Fig. 3(e and f) shows transmission electron micrographs of 0.6 and 1 mol% Nb-modified PLSZFT, respectively. Most of the samples had an average grain size of 1–2 μm but no distinct grain boundaries can be observed and nearly dense compacts of 98% theoretical density are obtained. A fairly uniform microstructure has been observed in Nb-modified PLSZFT ceramics as illustrated in Fig. 3. The grain growth enhanced as Nb content increased up to 1 mol% (2.07 μm). The rapid grain growth up to 1 mol% Nb was evidenced by the pore-free grains along the grain boundaries and within grains. It appeared that 1 mol% Nb is at the threshold of the grain growth mechanism. In good agreement with the literature, a similar trend was observed with Nb doping in PBZT relaxor ferroelectric ceramic system [16]. Apparent densities of sintered ceramics were measured using the Archimedes method. The density of PLSZFNT was higher than undoped PLZT and PLSZFT ceramics. The reasons for enhanced density and small grain size could be due to the addition of excess PbO and the influence of Nb. The apparent density increased till 1 mol% Nb constantly in PLSZFT nanoceramics when compared to that of undoped compositions. Microstructural studies revealed that pore-free and tightly bound grains promoted the densification of the ceramics. The grain coarsening process at lower temperature is negligible and a uniform microstructure is obtained. The microstructural analysis revealed the mixture of fine and coarse grains bounded uniformly. The increasing sintering temperature and the chemical diffusion of multiple dopants (La^{3+}, Sr^{2+} and Nb^{5+}) leading to lead vacancies while Fe^{3+} leading to oxygen vacancies. The oxygen vacancies are being compensated by the donor doping and distribution of both A-site and B-site vacancies in the lattice [17]. The distribution of A-site and B-site vacancies has been studied extensively by Hardtl and Hennings [18]. In our investigation, the lead vacancies [19] caused by the presence of La^{3+} and Sr^{2+} cations play a significant part in the microstructural homogenization of PLSZFNT nanoceramics. The increasing compositional homogenization produced by greater atomic diffusion in PLSZFNT could be attributed to the increasing concentration of lead vacancies caused by the sintering temperature which may have caused the rapid movement of the domain walls. TEM studies for calcined

Table 2
Tolerance factor data

Composition	Tolerance factor, t
PLZT	1.10
PLSZFT	1.19
PLSZFNT	1.00

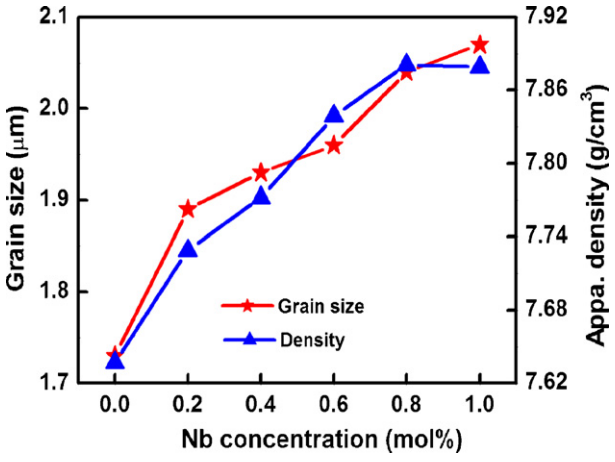

Fig. 2. Average grain size variation and apparent density of undoped and Nb-modified PLSZFT nanoceramics, respectively.

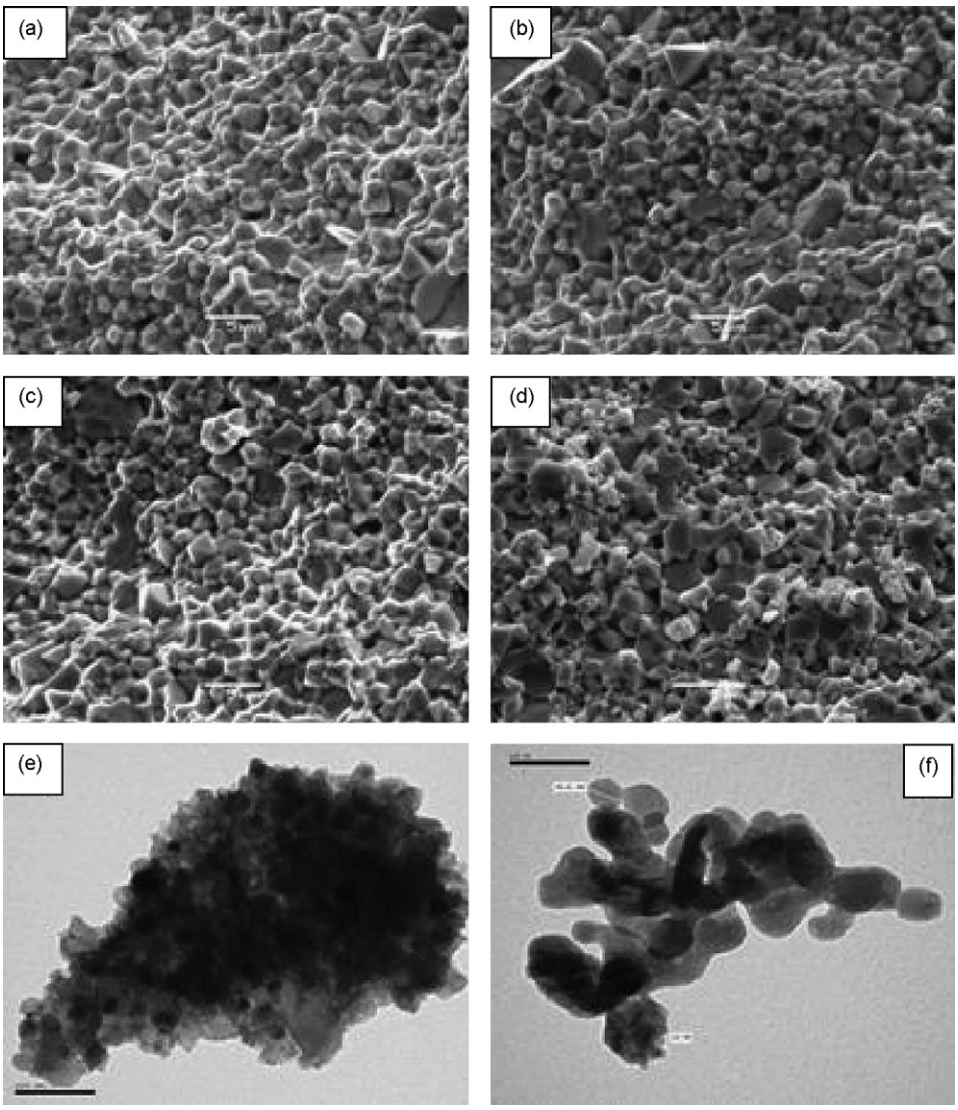

Fig. 3. (a–d) Scanning electron micrographs (fractured surfaces) of 0.2, 0.4, 0.6 and 1 mol% Nb-modified PLSZFT, respectively, and (e and f) transmission electron micrographs of 0.6 and 1 mol% Nb-modified PLSZFT, respectively.

powders revealed that fine and semi-agglomerated nanoceramic powders with particle size ranging from 16 to 63 nm. The donor Nb modification (0–1 mol%) in the PLSZFT near MPB 54/46 remarkably increased the grain growth and density. We are systematically studying different dopants (donor, isovalent and/or acceptor) with different Zr/Ti ratios near MPB to find out the effect of dopant nature and its concentration on different properties. In our previous study [20], we found that grain sizes were larger than the grain sizes of undoped (PLSZFT) due to the variation of La (donor), Fe (acceptor) and Zr/Ti ratios in these compositions. In our study, it is observed that donor Nb content resulted in small grains with an increasing trend of grain growth.

3.4. Dielectric response of undoped and Nb-modified PLSZFT nanoceramics

Fig. 4 shows (a) room temperature dielectric constant (ε_{RT}), (b) Curie temperature (T_c), (c) dielectric loss ($\tan\delta_{RT}$) and (d) dielectric maximum (ε_{Tc}) of undoped and Nb-modified PLSZFT nanoceramics, respectively. The maximum dielectric response was observed in 1 mol% Nb (2862). The dielectric constant is proportionally dependent on the grain size with the sintering temperature. The increasing Nb content led to a significant increase in the dielectric constant when compared to undoped composition. The dielectric constant showed an increasing trend which is quite contrary to the results reported by Klissurska et al. [21] who found decreasing ε with increasing Nb content in thin films. The Curie temperature (T_c) decreases with increasing Nb content. This trend is well in agreement with the results reported for PNZT ceramics with compositions in the tetragonal phase [22]. It is well known that Nb^{5+} preferentially substitutes the Zr-site which will shift the composition towards Ti-rich side with low T_c temperatures. The microstructure parameters influence the electrical and mechanical properties of the ceramics [23]. The dielectric and piezoelectric properties of PZT and PLZT ceramics are influenced by domain-wall existence and its movement [24]. The dopants and their concentrations in Ferroelectric tetragonal (FE_{TET}) domain orientation influence the domain-wall motion. The increase in dielectric constant could be ascribed to the modification of A-site cations (La^{3+} and Sr^{2+}) donor and isovalent dopant substituting Pb^{2+} and donor Nb^{5+} substituting Zr^{4+}/Ti^{4+} at B-site, and thereby reducing the

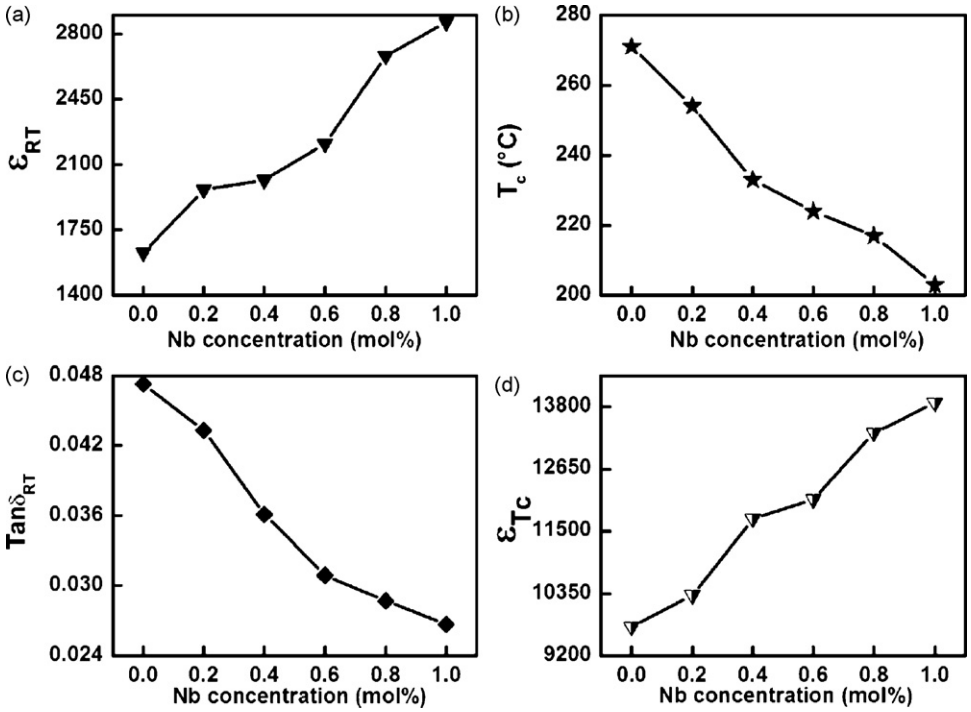

Fig. 4. (a) Room temperature dielectric constant (ε_{RT}), (b) Curie temperature (T_c), (c) dielectric loss (tan δ_{RT}) and (d) dielectric maximum (ε_{Tc}) of undoped and Nb-modified PLSZFT nanoceramics, respectively.

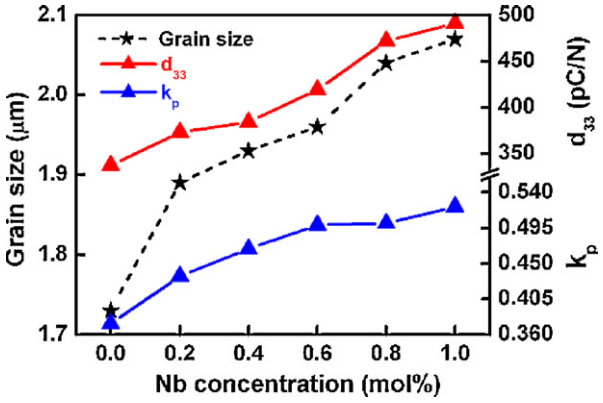

Fig. 5. Piezoelectric properties (piezoelectric charge coefficient (d_{33}) and piezoelectric planar coupling coefficient (k_p)) of undoped and Nb-modified PLSZFT nanoceramics, respectively.

oxygen vacancies created by acceptor Fe^{3+} in the perovskite lattice. The dielectric loss (tan δ_{RT}) gradually decreased from undoped to 1 mol% Nb in the series. It is reported that Nb doping unambiguously induces a softening effect and higher dielectric constant, higher piezoelectric coefficients and electromechanical coupling coefficients can be obtained [25] and our results are consistent with this observation reported in the literature.

3.5. Piezoelectric properties of undoped and Nb-modified PLSZFT nanoceramics

Fig. 5 shows the piezoelectric properties (piezoelectric charge coefficient (d_{33}), and piezoelectric planar coupling coefficient (k_p)) of undoped and Nb-modified PLSZFT nanoceramics, respectively. It is observed that d_{33} and k_p enhanced with increasing Nb modification in PLSZFT series. The piezoelectric properties depend on many factors namely compositional dependence of intrinsic properties, domain-wall movement, nature, amount of dopant concentrations, etc. The piezoelectric charge coefficient, d_{33} = 491 pC/N and piezoelectric planar coupling coefficient, k_p = 0.522 exhibited optimum values at 1 mol% Nb. The enhanced piezoelectric properties may be due to the donor dopants which reduces the concentration of the intrinsic oxygen vacancies created due to PbO evaporation during the sintering of PZT ceramics and introduces lead vacancies to maintain the charge neutrality [26]. It is evident that dense ceramics would have better piezoelectric properties. The combinatory influence of donor, isovalent and acceptor dopants have induced the polarization and enhanced the mobility of ferroelectric domains which facilitated grain growth enhancement in the nanoceramics influencing domain orientation resulting in enhancement of electro-mechanical activity. As a result, donor Nb modification in PLSZFT lattice has remarkably influenced the corresponding piezoelectric properties and high piezoelectric coefficients were achieved [27].

4. Conclusion

The structural, dielectric and electromechanical properties of donor Nb^{5+}-modified PLSZFT ceramic system had been studied. In Nb-modified PLSZFT ceramics, microstructural evolution and nucleation enhanced the crystallization process. The constituent dopants helped in achieving dense ceramics in the tetragonal symmetry supported by tolerance factor. The tolerance factor (t = 1.00) indicates an ideal and stable tetragonal structure of PLSZFNT lattice. X-ray diffraction results exhibited that Nb modification resulted in chemical homogeneity and diffusivity in PLSZFT nanoceramics supported by tolerance factor. Nb modification resulted in small grain size and increasing Nb content resulted in enhancement of grain growth which in turn enhanced dielectric and piezoelectric properties. The optimum dielectric response and electromechanical properties of 1 mol% Nb-modified PLSZFT nanoceramic composition could be suitable for possible sensor and actuator applications.

Acknowledgments

The authors would like to thank University of Concepcion, Chile and Andhra University, India. We would also like to thank Mr. Ranganathan, Mr. Krishnamurthy and Ms. C.N. Devi for their technical support, discussions and valuable suggestions extended during this work.

References

[1] B. Jaffe, W.R. Cook, H. Jaffe, Piezoelectric Ceramics, Academic Press, London, 1971, pp. 100–218.
[2] K. Kakegawa, O. Matoumaga, T. Kato, Y. Sasaki, J. Am. Ceram. Soc. 78 (1995) 1071.
[3] J.F. Meng, R.S. Katiyar, G.T. Zou, X.H. Wang, Phys. Status Solidi a 164 (1997) 851.
[4] Th. Michael, S. Trimper, J.M. Wesselinowa, Phys. Rev. B 74 (2006) 214113.
[5] K. Ramam, V. Miguel, Eur. Phys. J. Appl. Phys. 35 (2006) 43.
[6] H. Zheng, I.M. Reaney, W.E. Lee, N. Jones, H. Thomas, J. Eur. Ceram. Soc. 21 (2001) 1371.
[7] S. Sriram, M. Bhaskaran, A.S. Holland, K.T. Short, B.A. Latella, J. Appl. Phys. 101 (2007) 104910.
[8] G.H. Maher, J. Am. Ceram. Soc. 66 (1983) 408.
[9] R. Rai, S. Sharma, N.C. Soni, R.N.P. Choudhary, Phys. B: Condens. Matter 382 (2) (2006) 252.
[10] K. Ramam, M. Lopez, Phys. Status Solidi (a) 203 (15) (2006) 3852.
[11] R.D. Shannon, Acta Cryst. A32 (1976) 751.
[12] A. Mabud, J. Appl. Cryst. 13 (1980) 211.
[13] W.Z. Zhu, A. Kholkin, P.Q. Mantas, J.L. Baptista, J. Mater. Sci. 36 (2001) 4089.
[14] Y. Xu, Ferroelectric Materials and Their Applications, Amsterdam, North-Holland, 1991, pp. 101–105.
[15] R.S. Roth, J. Res. Natl. Bur. Stand. 58 (1957) 75.
[16] M.J. Pan, R.J. Rayne, B.A. Bender, J. Electroceram. 14 (2005) 139.
[17] M. Es-Souni, A. Piorra, C.H. Solterbeck, S. Iakovlev, M. Abed, J. Electroceram. 9 (2002) 125.
[18] K.H. Hardtl, D. Hennings, J. Am. Ceram. Soc. 55 (5) (1972) 230.
[19] L.A. Celi, A.C. Caballero, M. Villegas, J.D. Frutos, J.F. Fernandez, Ferroelectrics 270 (2002) 105.
[20] K. Ramam, Marta Lopez, J. Mater. Sci.: Mater. Electron. (2007), doi:10.1007/s10854-007-9492-1 Online First.
[21] R.D. Klissurska, K.G. Brooks, I.M. Reaney, C. Pawlaczyk, M. Kosec, N. Setter, J. Am. Ceram. Soc. 78 (1995) 1513.
[22] C.O. Paiva-Santos, C.F. Oliveira, W.C. Las, M.A. Zaghete, J.A. Varela, M. Cilense, Mater. Res. Bull. 35 (2000) 15.
[23] K. Ramam, M. Lopez, J. Eur. Ceram. Soc. 27 (2007) 3141.
[24] Q.M. Zhang, H. Wang, N. Kim, L.E. Cross, J. Appl. Phys. 75 (1) (1994) 454.
[25] L. Eyraud, B. Guiffard, L. Lebrun, D. Guyomar, Ferroelectrics 330 (2006) 51.
[26] S.B. Majumder, B. Roy, R.S. Katiyar, S.B. Krupanidhi, J. Appl. Phys. 90 (2001) 2975.
[27] R.S. Nasar, M. Cerqueira, E. Longo, J.A. Varela, A. Beltran, J. Eur. Ceram. Soc. 22 (2002) 209.